Recent Developments on Industrial Applications of MHD at the University of Bologna

F. Negrini, C.A. Borghi, P.G. Albano, M. Breschi, F. Colli, A. Cristofolini, M. Fabbri, F.Galante, A. Morandi, P.L. Ribani

Department of Electrical Engineering, University of Bologna, Viale Risorgimento 2, 40136 Bologna, Italy

***Abstract*— Some recent activities, developed in the Department of Electrical Engineering of the University of Bologna with the aim to analyse different electric power applications of MHD Sciences, are reported.**

I. Introduction

Some new activities started in the Department of Electrical Engineering of the University of Bologna, with the aim to analyze different electric power applications of MHD Sciences and superconducting technologies. In this communication some information concerning MHD processing of materials and SF6 circuit breakers, are given.

The "Electromagnetic Processing of Materials (EPM)" is based on both MHD and Process Metallurgy. Application of electromagnetic forces to materials processing, which constitutes EPM, has been recognized as an edge technology, especially in the fields of steelmaking and advanced materials processing. In metallurgy many process involve the handling of liquid metal in a technologically difficult environment. It's apparent that by use of the MHD effects, that is by a suitable application of the **J**×**B** and magnetization forces, improvements in existing processes or new solutions of old problems may be achieved. Examples of the successful application of the MHD processes in the metallurgical processing are electromagnetic stirring, braking and shaping. A new effort is requested to apply these technologies in steelmaking process.

II. Electromagnetic Processing of Materials

A typical EPM application in metallurgical processes is the control of the molten steel flow in the continuous casting mold. In fact, the surface and internal defects in cast slabs are closely related to the fluid flow of the molten steel. Numerical analysis on the steel flow inside the mold, in presence of an external magnetic field, has been carried out.

2.1 Numerical simulation of molten steel flow

The present work describes the three-dimensional numerical simulation of the molten steel flow in continuous casting mold at No. 3 caster at Chiba Works, Kawasaki Steel Corporation. The first objective is to study the influence of the imposed static magnetic field on the flow pattern, with the injections of Argon bubbles. The second aim is to find a representative diameter of the injected bubbles, which can simulate the surface velocity of molten steel flow by using the computational fluid dynamics code FLUENT™.

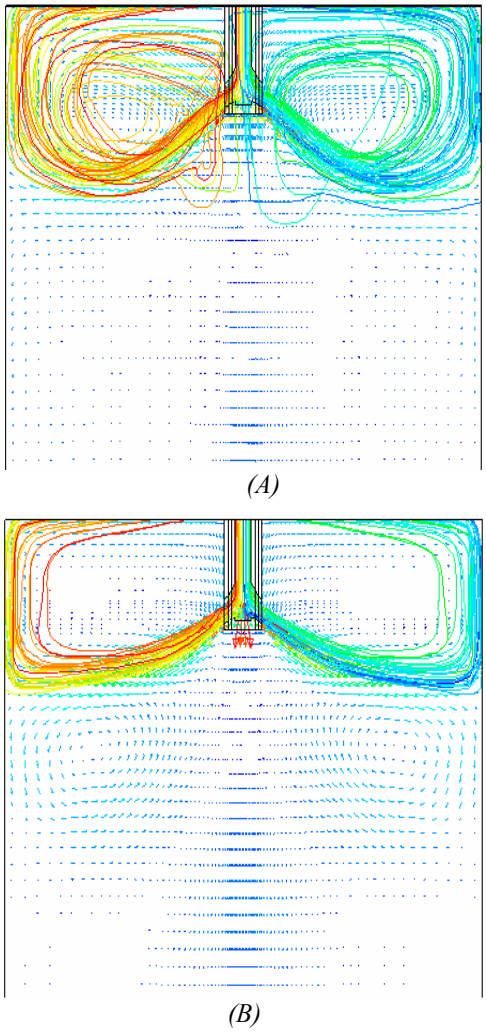

(A)

(B)

Fig. 1 - Comparison of velocity fields and bubbles trajectories on the central slab face for different conditions: A) without flux density field, Argon bubbles diameter of 0.5 mm; B) with flux density field, Argon bubbles diameter of 0.5 mm.

The governing equations for the three-dimensional incompressible viscous flow in a static magnetic field, are the Navier-Stokes equation, the Maxwell equations and the Ohm's law. The calculation were performed using a three-dimensional Cartesian mesh with a grid number of 134160 cells (86×13×120). Turbulence has been considered by using the k-ε standard model. To predict the trajectories of the injected Argon bubbles, the Phase Dispersed Model was used. The external magnetic field distribution, for the MHD analysis, was calculated by J-MAG program and fitted to only a horizontal component, that is the direction of mold thickness. In the design of

the FC Mold considered, two pairs of electric magnets, above and below the SEN, impose an horizontal static magnetic field distribution, with a maximum value of 0.31T. Two different cases are reported with Argon bubble diameter of 0.5 mm, with and without magnetic field imposition (Figure 1). The dimensions of the casting mold in this calculation are 1600 mm width and 260 mm thickness. The submerged entry nozzle (SEN) is two ports type. The throughput is 4.7 ton/min.

The influence of the injected Argon bubbles diameter on the molten steel surface was calculated through the simulation. In the case without magnetic field imposition (Figure 2.A), the injection of Argon bubbles with 0.5 mm diameter increases the velocity, while the injections of Argon bubbles with 1 mm and 2 mm diameters have a decreasing effect. In the case with magnetic field imposition (Figure 2.B) the velocity, in case without Argon injection, is negative, that is directed toward the narrow face. The decreasing of the diameter of the injected bubbles increases the change of direction of the flow.

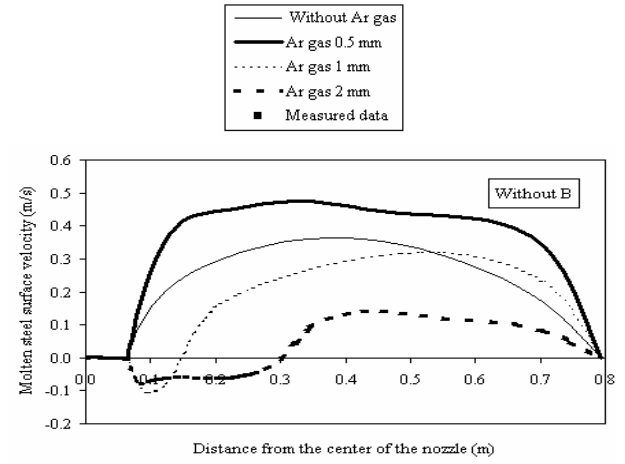

(A)

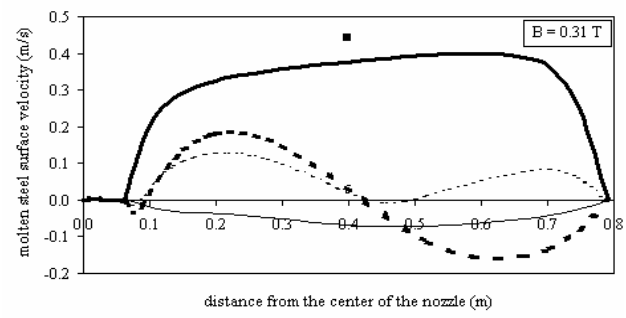

(B)

Fig. 2 - Effect of Argon injection on molten steel surface velocity distribution along the slab central line: A) without magnetic field imposition, B) with magnetic field imposition. Positive velocity is toward the nozzle.

As can be seen from Figure 2.B, the molten steel surface velocity, for the case with injected Argon bubbles with 0.5 mm diameter (at 3.7 m/s), is the nearest to the measured data of No. 3 Continuos Casting machine. Moreover, the imposition of the magnetic field, in the suitable case of 0.5 mm, gives an effect of surface velocity reduction of 22% that is similar to what was previously found by Kawasaki Steel Company researchers.

2.2 Influence of Electro-Magnetic Stirring on the Boundary Layer of a Molten Steel Pool.

In the case of in-mold stirring, the AC field is generated by the travelling field generated by a linear motor (in case of slabs) or a rotational motor (in case of blooms and billets). The electromagnetic force is generated only by the electromagnetic field: the induced current and the magnetic field interact mutually to generate the electromagnetic force in the molten metal. This EM technique is aimed at controlling the different velocity components and the flow pattern is optimized to expel as much as possible the impurities such as non-metallic inclusions, CO bubbles and Argon blow-holes. Moreover, a particular attention is paid to the control of the velocity of the discharged flow from the nozzle.

The behavior of the molten steel can be predicted by coupling Maxwell's equations, equation of continuity and Navier-Stokes equation for incompressible fluids. The numerical simulation was carried out using the code FLUENT™. As the flux pattern in the continuous casting is turbulent, the Large Eddy Simulation (LES), and RNG k-ε models were considered as turbulence physical models. These models were tested on an illustrative case: a molten steel pool 10cm×10cm with a moving wall. The comparison among the obtained velocity distributions and the experimental data is depicted in Fig.3, where the x-axis is parallel to the moving wall and centered on the pool.

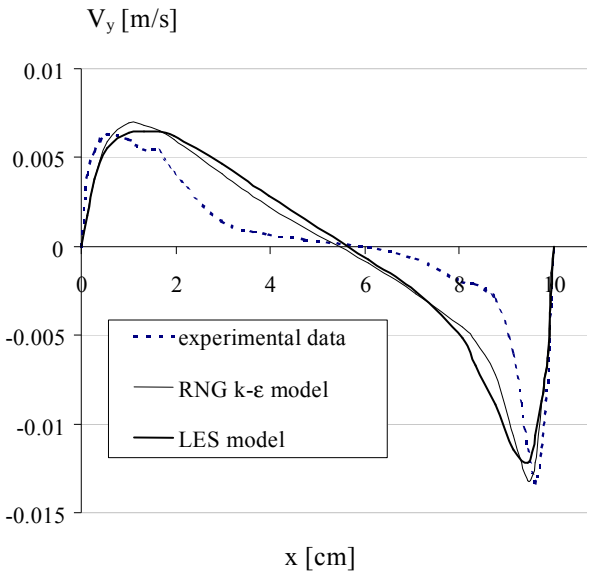

Fig. 3 – Comparison among the velocity profiles obtained considering RNGk-ε and LES as turbulence models and the experimental data for a test case (a molten steel pool with a moving wall).

Satisfactory results have been reached with a 50×50 mesh grid. Then the analysis of an In-mold EMS was performed: a molten steel pool (simulating the mold of a continuous caster for billets) affected by electromagnetic force was considered. The velocity patterns obtained are shown in Fig.4. In both cases the maximum value of the velocity was the same.

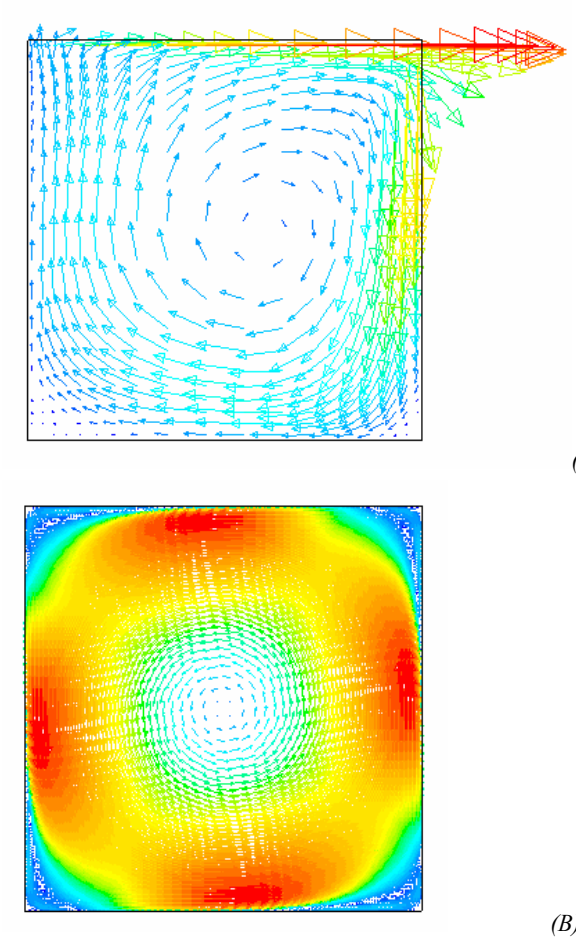

(A)

(B)

Fig 4 – Calculated velocity distribution inside the mold of a continuous caster for billets (A) when a moving wall is assumed, (B) when electromagnetic force is applied.

The objective of the research was the evaluation of the influence of electromagnetic force on the boundary layer of a molten steel pool. It's known that, when a slab is considered, in the boundary layer EMS modifies the velocity distribution. In particular the molten steel velocity near the wall changes from a pseudo-linear distribution to a parabolic one. This change of the velocity gradient generates a force acting on the inclusions and particles, which are present in the molten steel. Actually such a force, called Saffmann force, pushing the particle toward the center of the pool, depends non-linearly from the gradient of the velocity. Furthermore, when the Saffmann force passes a threshold value, the particle is removed from the wall and then from the solidifying shell.

2.3 Removal of SiC inclusions in molten Aluminum using magnetization force

During several years, numerous results have been achieved regarding the separation of inclusion in a molten metal. However, the peculiar aspect of our work stands in the definition of experimental parameters to conduct the analysis of the obtained results. In fact, the SiC inclusions in the molten aluminum are rather smaller than the Al_2O_3 ones in a molten steel and this fact causes a big statistical variations to arise in the collected data, so that their analysis must be carried out by the use of statistical methods. Under the hypothesis of homogeneous distribution of the particles, gaussian distribution and uniform variance of the collected data, the Student's t-test has been applied to evaluate the statistical error, in order to affirm that the observed removal of inclusions is not due to it, but only to the effect of the applied magnetic field.

First of all, the hypothesis of spherical SiC particles all having the same diameter, under which several theoretical works have been developed, has been tested. Two parameters d (mean value of the particles diameter) and C_s (ratio between the maximum and minimum dimensions of the particles) have been evaluated for a casually extracted section in a not-treated sample, shown in Fig. 5.a. The result of the micrographic observation (Fig. 5.b) has lead to determine the error made in assuming the spherical shape of the particles and a constant value for their diameter. In fact, the mean value for C_s in the case of perfect identical spheres should be 1, being instead 0.683 for the examined inclusions. On the other hand the ratio between the standard variation of d and its mean value represent an error factor for the assumption of a constant value for the diameter, that has be found to be 31%.

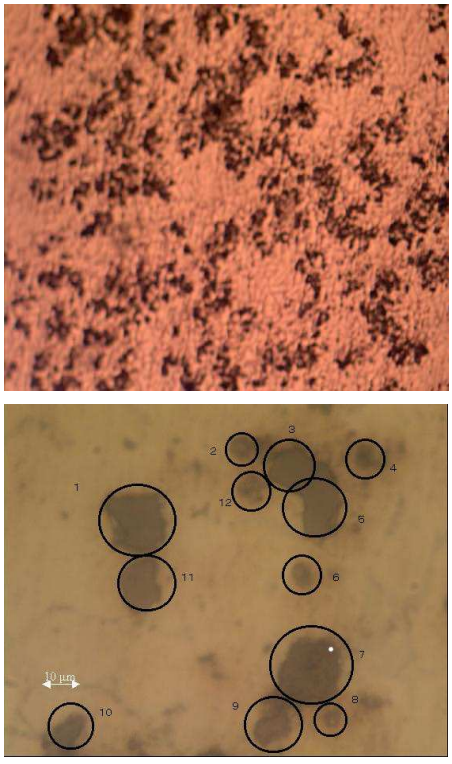

(A)

(B)

Fig. 5 - A) Homogeneous distribution of the inclusions, (the base length is 4.6 mm); B) Geometrical shape of the particles.

Under the above mentioned hypothesis the comparison has been carried out by the Student's t-test using as analytical parameters the number of inclusions per unity of area of a generic section for a not-treated samples and the number of inclusions per unity of area in a bottom section for the treated ones. In order to obtain such a comparison, five samples have been completely melted and kept for 1 h at 12 T and than slowly cooled, according to the thermal treatment shown in Fig. 6. The 12 T magnetic field was generated using a superconducting

magnet, which had a room temperature air bore of 50 mm in diameter. Fig. 7 shows a sharp segregation line between the zones at high and low number of inclusions.

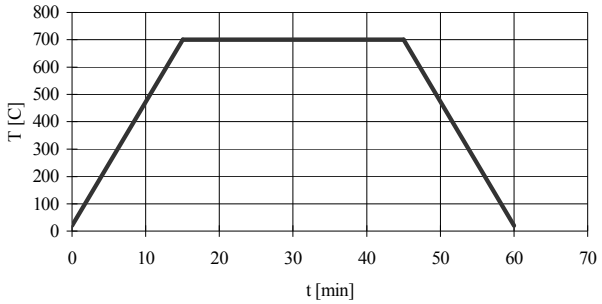

Fig. 6 – Thermal cycle for the treated samples; the magnetic field is applied all the period long.

Fig. 7 – Segregation line of the treated sample (the base length is 4.6 mm).

A statistical analysis on five aluminum samples has been conducted, from which SiC inclusions have been removed using a 12 T static magnetic field, and the presence of a boundary line between the pure zone and the segregated one has been observed. In the hypotheses of spherical particles and their uniform distribution, has been found that:

- the segregation effect, in terms of number of inclusion in the bottom of the sample is not due only to a statistical variation, but has to be considered as an effect of the applied field;
- the boundary line lays at a value of height proportional by 0.20 to the length of the sample, with a 15% error;
- the variation distribution of the particles around the boundary line lays within 15%.

III. Analysis of the discharge in an SF_6 circuit breaker

A fully implicit method for the numerical solution of the model for the analysis of the discharge in an SF_6 circuit breaker has been developed. The fluid dynamics is defined by the Navier Stokes equations for viscous and compressible flows. The continuity equations for mass, momentum and energy, and the state equations of gas are expressed as follows:

$$\frac{\partial \mathbf{U}}{\partial t} + \nabla \cdot \mathbf{F} = \mathbf{Q} \qquad (1)$$

$$p = p(\rho, T); \quad e_i = e_i(\rho, T) \qquad (2)$$

where ρ is the specific mass and e_i is the specific internal energy of the fluid. The quantities **U**, **F**, **Q** are defined as:

$$\mathbf{U} = \begin{vmatrix} \rho \\ \rho \mathbf{u} \\ e_i \end{vmatrix}, \quad \mathbf{F} = \begin{vmatrix} \rho \mathbf{u} \\ \rho \mathbf{u}\mathbf{u} + p\mathbf{I} - \boldsymbol{\tau} \\ e_i \mathbf{u} - \boldsymbol{\tau} \cdot \mathbf{u} - k \nabla T \end{vmatrix}, \quad \mathbf{Q} = \begin{vmatrix} 0 \\ \mathbf{J} \times \mathbf{B} \\ J^2/\sigma + \dot{R} \end{vmatrix}$$

Here the radiation term $\dot{R}$, the gas and the plasma conductivity σ are derived as a function of temperature and pressure, under the assumption of local thermal equilibrium.

From the Maxwell equations and Ohm's law, the governing equation for magnetic flux density **B** can be obtained:

$$\frac{\partial \mathbf{B}}{\partial t} = -\nabla \times \left(\frac{1}{\mu_0 \sigma} \nabla \times \mathbf{B} \right) + \nabla \times (\mathbf{u} \times \mathbf{B}) \qquad (3)$$

3.1 Numerical Method

A two-dimensional axis-symmetrical discharge model has been considered. The current density **J** and the gas velocity **u** are assumed to lie on the r-z plane. The magnetic flux density **B** generated by **J** is perpendicular to this plane. A fully implicit method has been developed for the solution of the magnetohydrodynamic problem. The discretization in the space and time is performed separately. In order to generate the mesh, an automatic procedure computing the Dirichlet tessellation of the calculation domain has been adopted. Joining contiguous points P by edges, a triangulation of the plane is obtained. It can be demonstrated that the triangulation is the Delaunay triangulation of the plane.

3.1.1 Fluid dynamic problem discretization

A cell-centered finite volume formulation is adopted for the spatial discretization of the fluid dynamics. The control volume for each point P_i is constituted by its Voronoi polygon. Integrating (1) over the control volume Ω_i, the following relation is obtained:

$$\frac{\partial}{\partial t} \int_{\Omega_i} \mathbf{U} \, dV + \sum \Phi_{\Gamma i}[\mathbf{F}] = \int_{\Omega_i} \mathbf{Q} \, dV \qquad (4)$$

where $\Phi_{\Gamma i}[\mathbf{F}]$ is the flux of **F** across the side of the control volume.

In order to avoid discretization inconsistencies, fluxes through sides are evaluated once at the beginning of each time step. A flux is constituted of a convection and a diffusion component, except the mass flux, where the diffusive term is not present. Convective fluxes are evaluated with reference to the velocity of the upwind point. Thus, when evaluating the flux through the edge between the P_i and P_k tiles shown in Fig. 8, the velocity normal components $u_{n,i} = \mathbf{u}_i \cdot \mathbf{n}_i$ and $u_{n,k} = \mathbf{u}_k \cdot \mathbf{n}_k$ are evaluated. Afterward convective fluxes are computed utilizing the positive normal component of the velocity.

In order to calculate the diffusive fluxes, the spatial first derivatives on each edge are to be evaluated. The derivatives on the edge are calculated as the mean value of

the derivatives in the two triangles with P_i and P_k as vertex (see Fig. 8). Over the triangles the unknown quantities are assumed to be linear. This procedure yields the derivatives in the normal and tangential direction to the edge considered. The latter is necessary in evaluating the viscous term in the momentum equation only. Pressure on the edges between the P_i and P_k tiles is calculated as the mean value of the pressure in P_i and P_k.

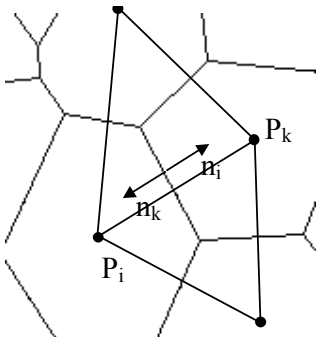

Fig. 8 - Control volumes for the fluid dynamics discretization.

3.1.2 Electrodynamic problem formulation

The discretization in space of the electrodynamic problem expressed by (3) has been carried out by means of a finite element method based on the weighted residual approach. The matrix relation obtained is:

$$\frac{\partial \boldsymbol{\varphi}}{\partial t} = \mathbf{K}\boldsymbol{\varphi} \tag{5}$$

where $\boldsymbol{\varphi}$ is the vector of the nodal values of the unknown rB_φ. In order to evaluate the electromagnetic source terms in momentum and energy equation of fluid dynamics, the current density has to be evaluated. This is done utilizing the Ampere law:

$$J_r = -\frac{1}{\mu_0 r}\frac{\partial (rB_\varphi)}{\partial z} \tag{6.a}$$

$$J_z = \frac{1}{\mu_0 r}\frac{\partial (rB_\varphi)}{\partial r} \tag{6.b}$$

The coefficient matrix $\mathbf{K}$ is the sum of $\mathbf{K}_{diff}$ and $\mathbf{K}_{conv}$, derived from the discretization of the diffusive term $\nabla\times[\nabla\times\mathbf{B}/(\mu_0\sigma)]$ and the convective term $\nabla\times(\mathbf{u}\times\mathbf{B})$ of (3) respectively. The expressions of $\mathbf{K}_{diff}$ and $\mathbf{K}_{conv}$ are:

$$\mathbf{K}_{diff} = \frac{1}{\mu_0}\int_\Omega \nabla\mathbf{W}^T \frac{1}{r\sigma}\nabla\mathbf{N}\,d\Omega \tag{7.a}$$

$$\mathbf{K}_{conv} = \int_\Omega \mathbf{W}\frac{1}{r}\mathbf{u}^T\nabla\mathbf{N}\,d\Omega \tag{7.b}$$

where $\mathbf{N}$ and $\mathbf{W}$ are the shape function and the weighting function vector respectively. An asymmetric function is chosen to increase the residual weighting in the upstream region and to reduce it in the downstream region. For a generic triangular element with vertexes i, j, k, the weighting function W_i assumes the following form:

$$W_i = N_i + 4\alpha_{ij}N_iN_j + 4\alpha_{ik}N_iN_k \tag{8}$$

The parameter α_{ij} and α_{ik} are calculated as follows:

$$\alpha_{ij} = \coth(Re_{m\Delta_{ij}}/2) - 2/Re_{m\Delta ij} \qquad Re_{m\Delta ij} = \mu_0\sigma u_{ij}\Delta_{ij}$$

$$\alpha_{ik} = \coth(Re_{m\Delta_{ik}}/2) - 2/Re_{m\Delta ik} \qquad Re_{m\Delta ik} = \mu_0\sigma u_{ik}\Delta_{ik}$$

where Δ_{ij}, Δ_{ik} are the lengths of the sides i-j and i-k of the triangle. u_{ij}, u_{ik} are the flow velocity components along the $\mathbf{i}_{ij}$ and $\mathbf{i}_{ik}$ directions, as shown in Fig. 9.

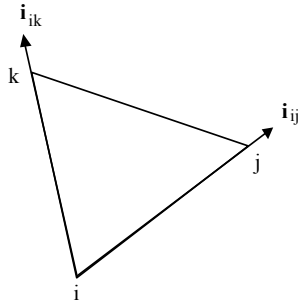

Fig. 9 - Triangular grid element.

The boundary conditions needed to solve (3) can be obtained from the Ampere law. Defining I as the total current flowing in the discharge, in a cylindrical symmetry boundary they are:

$$\varphi = rB_\varphi = \mu_0\frac{I}{2\pi} \tag{9}$$

on the external surface of the discharge.

Time integration is performed by means of a two-time step algorithm. Different approaches have been utilised to couple the fluid dynamics with the electrodynamics. A first way to perform the coupling is to solve the non-linear system obtained at each time step:

$$\mathbf{F}\left(\mathbf{f}^{(n)}\right) = 0 \tag{10}$$

where the vector $\mathbf{f}^{(n)}$ is formed by the nodal values of the two velocity component u_r and u_z, the pressure p, the temperature T and the azimuthal component of the magnetic flux density rB_φ. An inexact Newton method is utilized to solve the system. Alternatively, at each time step fluid dynamics and electrodynamics can be solved separately and iteratively coupled until convergence is reached. The second approach has proved to be more efficient in terms of computing time. Diagonal, ILU and approximate inverse preconditioner have been utilised to enhance the convergence rate of the solution.

3.2 Applications

An arc discharge during the high current phase in an SF_6 circuit breaker has been analysed. A scheme of the contact region of the device is depicted in fig. 10. During a current interruption an arc develops between the two contacts when they are opened. In a typical SF_6 discharge in a circuit breaker, conductivity ranges between 0 and 15000 S/m, and the gas velocity can easily exceed 1000 m/s. A sinusoidal time varying current with an amplitude of $5\cdot10^3$ A and a frequency of 50 Hz is taken as source of the electrodynamic problem. The gas flow is caused by a pressure difference of 3 bar between the initial and the final section. The grid consists of 5096 nodes and 9682 triangles. The velocity, temperature and pressure distributions in the discharge are shown in Figs. 11(a), 11(b) and 11(c) respectively. Current lines are plotted in Fig. 11(d).

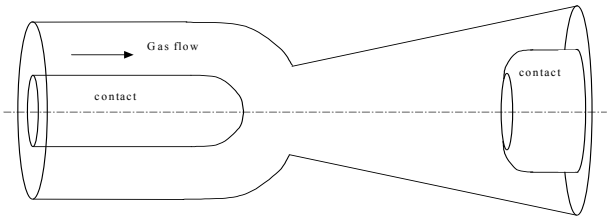

Fig. 10 – Scheme of the contact region in an SF_6 circuit breaker.

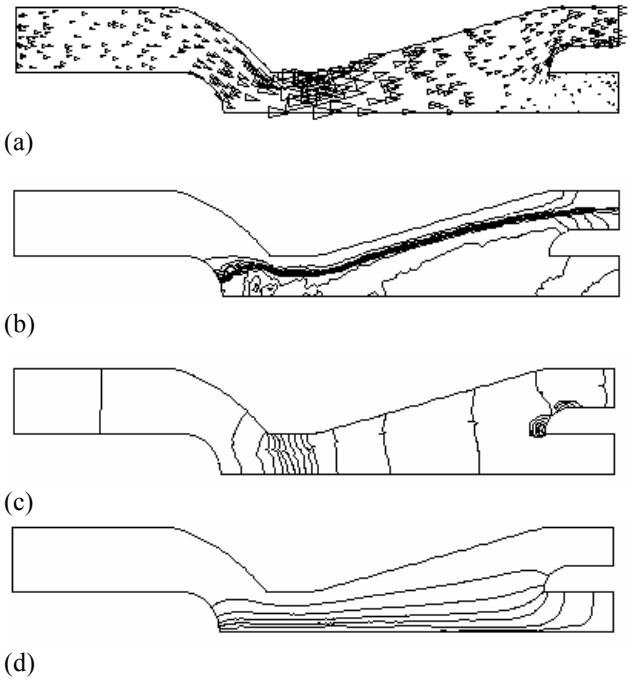

Fig. 11 – (a) Velocity distribution; (b) Temperature distribution: Temperature ranges between 300 and 27500 K; (c) Pressure distribution; (d) Current lines.

IV. RESISTIVITY EFFECTS IN A FUSION PLASMA LINEARIZED MODEL

In the framework of a research project on fusion plasma control, supported by the Ministry of Education of Italy, a research activity was started with the main goal of introducing a resistive plasma equation into the linear model of the CREATE_L code. This code, which was developed by the CREATE Consortium for utilization in the design of the controller of a Tokamak machine is actually based on an ideal non-resistive plasma model. The code has been validated with experimental results with reference to many Tokamak machines (TCV, FTU, JET). The obtained results were satisfactory but evidence was demonstrated that resistive effects are important.

A plasma current equation based on generalized Ohm's law, averaged on the discharge volume consistently with the assumptions of the CREATE_L model has been implemented into the CREATE_L code. The numerical results have been compared with experimental data obtained in TCV and FTU tokamak machines and qualitative agreement has been obtained. The research activity is still going on.

V. CONCLUSIONS

Some new activities which started in the Department of Electrical Engineering of the University of Bologna, with the aim to analyse different electric power applications of MHD Sciences and superconducting technologies, are reported.

Numerous other activities regarding MHD have been carried out during 1998/2001 resulting in the papers that are reported in the references.

REFERENCES

[1] C.A. Borghi, A. Cristofolini, "Magnetohydrodynamic Interaction in Plasmas with Magnetic Reynolds Number Near Unity", *Proc. of the 1998 Symposium on Advanced Energy Technology*, Sapporo, Japan, 2-4 February, pp. 423-430, 1998.

[2] A. Cristofolini, F. Negrini, M. Breschi, "Capture Processes in Superconducting HGMS", *Proc. of the 1998 Symposium on Advanced Energy Technology*, Sapporo, Japan, 2-4 February, pp. 129-136, 1998.

[3] C.A. Borghi, M. Fabbri, "Multi-Objective Global Optimization of SMES Design", *Proc. of the 8th International IGTE Symposium*, Graz, Austria, 21-24 September, pp. 20-25, 1998.

[4] C.A. Borghi, A. Cristofolini, M. Fabbri, "Study of the Design Model of a Liquid Metal Induction Pump", *IEEE Trans. Magn.*, 34, pp. 2956-2959, 1998.

[5] C.A. Borghi, M. Fabbri, "Iron Shielded MRI Optimization", *J PHYS III*, 3, pp. 343-348, 1998.

[6] C.A. Borghi, A. Cristofolini, "Investigation on the Magnetic Field Convection Effects in the Discharge in SF6", Records of the 1998 IEEE Int. Conf. on Plasma Sciences (Raileigh, North Carolina, 1-4 Giugno 1998) a cura di J. Gilligan, Conference Chair, pp. 198-198, Edited by the IEEE Nuclear and Plasma Sciences Society, Raileigh, North Carolina, 1998.

[7] C.A. Borghi, M. Fabbri, P. Di Barba, A. Savini, "Loney's Solenoid Multi-Objective Optimization Problem", *IEEE Trans. Magn.*, 35, n.3, pp. 1706-1709, 1999.

[8] C.A. Borghi, M. Fabbri, P.L. Ribani, "Design Optimization of a Micro-SMES Magnetic System", *IEEE Trans. Magn.*, 35, n.5, pp. 4275-4284, 1999.

[9] F. Negrini, M. Fabbri, P.L. Ribani, "Optimized Magnetic Design of a High Temperature Micro-SMES", *Int. J. Mod. Phys. B*, vol. 13, n.9-10, pp. 1351-1356, 1999.

[10] C.A. Borghi, A. Cristofolini, "A Fully Implicit Method for the Numerical Solution of the MHD Problem in an SF6 Discharge", *Proc. 26th IEEE Int. Conf. on Plasma Science*, Monterey, California, USA, 20-24 June, p. 216, 1999.

[11] C.A. Borghi, A. Cristofolini, "A Numerical Model for the Solution of the Magnetic Convection-Diffusion Equation at High Magnetic Reynolds Numbers", *Proc. 26th IEEE International Conference on Plasma Science*, Monterey, California, USA, 20-24 June, p. 215, 1999.

[12] F. Negrini, A. Cristofolini, M. Fabbri, P.L. Ribani, P.G. Albano, "Electromagnetic Shaping of a Liquid Metal Jet", *Proc. Int. Conf. on MHD Power Generation and High Temperature Technologies*, Beijing, PRC, 12-15 October, pp. 731-736, 1999.

[13] C.A. Borghi, A. Cristofolini, "Numerical Approach to a Magnetic Convection-Diffusion Problem at High Magnetic Reynolds Number", *Proc. Int. Conf. on MHD Power Generation and High Temperature Technologies*, Beijing, PRC, 12-15 October, pp. 521-523, 1999.

[14] F. Negrini, M. Fabbri, A. Cristofolini, P.L. Ribani, "A Multi wire Model for Superconducting HGMS Filter", *Proc. Int. Conf. on MHD Power Generation and High Temperature Technologies*, Beijing, PRC, 12-15 October, pp. 715-720, 1999.

[15] F. Negrini, P.L. Ribani, M. Breschi, L. Bottura, "Electromagnetic analysis of current distribution in multistrand superconducting cables", *Proc. 4th European Conf. on Applied Superconductivity,* Sitges (Spain), 14-17 September, p. 224, 1999.

[16] C.A. Borghi, M. Fabbri, P. Di Barba, A. Savini, "A Comparative Study of the Loney's Solenoid by Different Techniques of Global Optimization", *Int. J. of Applied Electromagnetics and Mechanics*, vol. 10, pp. 417-423, 1999.

[17] P.L. Ribani, N. Urbano, "Study on Figure-Eight-Shaped Coil Electrodynamic Suspension Magnetic Levitation Systems Without Cross-Connection", *IEEE Trans. Magn.*, vol. 36 (1), pp. 358-365, 2000.

[18] C.A. Borghi, V.A. Bityurin, A. Veefkind, "MHD Electrical Power Generationin in a T-Layer Plasma Flow", *IEEE Trans. Plasma Sci.*, 28 (3), pp. 1020-1028, 2000.

[19] F. Negrini, M. Fabbri, M. Zuccarini, E. Takeuchi, M. Tani, "Electromagnetic control of the meniscus shape during casting in a high frequency magnetic field", *Int. J. Energy Convers. Manag.*, vol. 41, pp. 1687-1701, 2000.

[20] C.A. Borghi, M. Fabbri, "Multimembered Evolution Strategies for the Global Optimization of Electromagnetic Devices", *Proc. of the 6th Int. Workshop on Optimization and Inverse Problems in Electromagnetism* (OIPE2000), Torino (Italy), 25-27 September, pp. 65-66, 2000.

[21] F. Negrini, P. G. Albano, C.A. Borghi, M. Breschi, D. Casadei, A. Cristofolini, M. Fabbri, G. Grandi, P. La Cascia, U. Reggiani, P.L. Ribani, C. Rossi, G. Serra, A. Tani, "Recent Developments on Micro-SMES systems Project at the University of Bologna", *Electrical Energy Storage Applications and Technologies Conf.* (EESAT2000), Orlando (Florida), 18-20 September, pp. 5A1-5A2, 2000.

[22] P.L. Ribani, M. Breschi, L. Bottura, A. Akhmetov, "A theoretical investigation on current imbalance in flat two-layer superconducting cables", *Proc. of the Workshop on Computation of tHermo-hydrAulic Transients in Superconductors* (CHATS-Y2K), Frascati (Italy), 6-8 September, p. EM1-2, 2000.

[23] P.L. Ribani, L. Bottura, M. Breschi, A. Akhmetov, "A continuum Model for Current Distribution in Rutherford Cables", *Proc. of the Applied Superconductivity Conf.* (ASC2000), Virginia Beach (Virginia), 17-22 September, p. 148, 2000.

[24] F. Negrini, L. Bigoni, E. Cereda, V. Ottoboni, P. La Cascia, P. L. Ribani, "Numerical Analysis of Hysteretic Losses on High Temperature Superconducting Coils", *Proc. of the Applied Superconductivity Conf.* (ASC2000), Virginia Beach (Virginia), 17-22 September, p. 149, 2000.

[25] C.A. Borghi, A. Cristofolini, "A Hybrid Implicit Numerical Method for the Analysis of the Magneto-Plasmadynamics in a Gas Discharge", *Proc. of the 9th Biennial IEEE Conf. on Electromagnetic field Computation* (CEFC-2000), Milwaukee (Wisconsin), 4-7 June, p. 229, 2000.

[26] L. Bottura, M. Breschi, M. Schneider, "Measurements of Magnetic Field Pattern in a Short LHC Dipole". *Proc. of the Applied Superconductivity Conf.* (ASC2000), Virginia Beach (Virginia), 17-22 September, p. 126, 2000.

[27] C.A. Borghi, P.L. Ribani, M. De Magistris, F. Villone, R. Albanese, M. Bagatin, G. Chitarin, F. Bellina, P. Bettini, A. Stella, F. Trevisan, G. Rubinacci, R. Martone, G. Marchiori, M. Guarnieri, F. Gnesotto, R. Fresa, A. Formisano, V. Coccorese, A. Pironti, M. Ariola, G. Ambrosino, "An Integrated Approach to the Control of Magnetically Confined Plasmas", *21st Symp. on Fusion Technology* (SOFT2000), Madrid (Spagna), 11-15 September, p. C01, 2000.

[28] F. Negrini, P.G. Albano, C.A. Borghi, A. Cristofolini, M. Fabbri, M. Zanetti, H. Shibata, Y. Kishimoto, "Applied MHD at the University of Bologna", *Proc. 4th Int. PAMIR Conf. on MagnetoHydroDynamic at Dawn of Third Millennium,* Presqu'ile de Giens (France), 18-22 September, pp. 161-166, 2000.

[29] C.A. Borghi, A. Cristofolini, "An Implicit Numerical Method for the Analysis of the Magneto-Plasmadynamics in a Gas Discharge", *Proc. of the XIII Int. Conf. on Gas Discharge and Their Applications* (GD2000), Glasgow (UK), 3-8 September, pp. 481-484, 2000.

[30] F. Negrini, L. Bigoni, E. Cereda, V. Ottoboni, P. La Cascia, P. L. Ribani, "Numerical Analysis of Hysteretic Losses in BiSCCO/Ag Tapes due to Transport Current and External Magnetic Field", *Int. J. Modern Physics B*, vol. 14, n.25-27, pp. 3165-3170, 2000.

[31] F. Negrini, A. Morandi, T. Nitta, S. Oshima, P. L. Ribani, "Experimental Analysis and Circuit Model of an Inductive Type High Temperature Superconducting Fault Current Limiter", *Int. J. Modern Physics B*, vol. 14, n.25-27, pp. 3171-3176, 2000.

[32] C.A. Borghi, P. L. Ribani, "Inclusion of resistivity in CREATE_L Model", in *models and Methods for Plasma Control in Fusion Devices* (MURST National Research Project 1999-2000 Final Report), pp.8-18, February 2001.

[33] C. A. Borghi, A. Cristofolini, "Numerical coupling of Fluid Dynamics and Electrodynamics for Gas Discharges Modelling", Accepted for *COMPUMAG'01*, Evian (France), 2-5 July 2001.

[34] C. A. Borghi, A. Cristofolini, "A Hybrid Implicit Numerical Method for the Analysis of the Magneto-Plasmadynamics in a Gas Discharge", Accepted for publication in *IEEE Trans. Magn.*, September 2001.

[35] F. Negrini, S. Asai, F. Colli, M. Fabbri, K. Sassa**, "**Removal of SiC inclusions in molten Aluminum using a 12 T static magnetic field**",** Accepted for *HIS-01*, Padua (Italy), 12-14 September 2001.

[36] F. Negrini, M. Fabbri, F. Galante, E. Takeuchi, T. Toh, "Influence of Electro-Magnetic Stirring on the Boundary Layer of a Molten Steel Pool", Accepted for *HIS-01*, Padua (Italy), 12-14 September 2001.